# DEM modelling of soil structures reinforced with geosynthetics

B. Chareyre
*LTDS, Ecole Centrale de Lyon, UMR CNRS 5513, Ecully, France*

P. Villard
*LIRIGM, Université J. Fourier, Grenoble, France*

ABSTRACT: The quasi-static behaviour of large soil/geosynthetic systems is investigated using DEM simulations in 2D. For this application, dynamic spar elements were introduced in the DEM for the modelling of the geosynthetic inclusions. Some computations are performed to predict the result of pull-out tests on geosynthetic anchorages. The results are in good agreement with experimental data regarding the main features of deformation and failure of the systems. This comparison shows that the DEM can provide quantitative information at a macroscopic scale (displacements, load at failure, ...), based on the concept of "macroscopic analogy" between the model and a real earth-work.

## 1 INTRODUCTION

In the fields of civil and geotechnical engineering, the construction techniques are getting more and more sophisticated and often include composite systems. Particularly, many reinforcement techniques associate a granular matrix (soil, concrete) with linear or planar inclusions (geosynthetics, fibers, concrete piles, steel rods). Modeling the mechanical behavior of such systems is generally complex since the geometry and governing mechanisms are strongly discontinuous. Traditional finite element methods, rooted in the concepts of continuum mechanics, may be unsuited in such cases (Villard et al. 2002). At the same time, significant advances in discrete modeling methods offer some opportunities for the numerical simulation of different types of composite systems (Mohammadi et al. 1998, Hentz et al. 2003). Those methods can be used to simulate soil-inclusion systems with respect to their discontinuous nature.

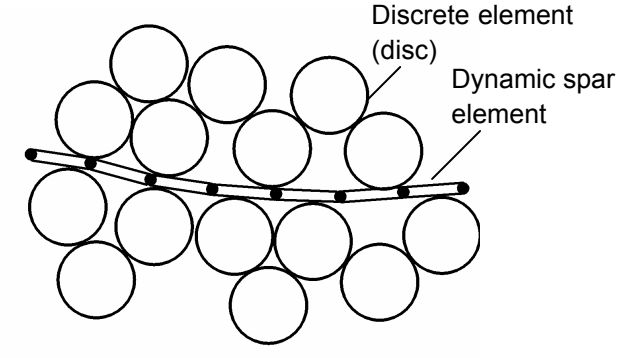


Figure 1. DEM coupled with Dynamic Spar Elements for the modeling of soil-inclusion problems.

This paper focus on the modeling of soil-geosynthetic systems (geosynthetics are generally planar polymeric inclusions), and present a comparison between true-scale pull-out tests on geosynthetic anchorages and DEM simulations in two dimensions.

## 2 MODELLING A GEOSYNTHETIC INCLUSION IN A GRANULAR MATERIAL

### 2.1 *Dynamic Spar Elements*

This section gives a brief overview of the dynamic spar elements (DSEM) that were proposed in Chareyre (2005) to simulate inclusions. The DSEM was initially designed specifically for the modeling of geosynthetic sheets, which have generally no bending strength. However, it is believed that the DSEM could equally apply to other types of inclusions, as bending strength could be introduced without difficulty.

In the DSEM, the motion of each element is determined based on the Newton's second law, using a centered finite difference scheme as in most discrete element methods (see Cundall and Strack 1979). The DSEM's specificities are mainly due to the shape and the deformability of the elements, the type of connection between them, and the inertial model.

### 2.2 *Discretization*

The inclusion is represented by a set of spar elements connected by nodes, as in Fig. 2.a. The length of the elements is considered variable, the axial de-

formation being accounted for by a variation of the distances between the nodes; the flexion of the inclusion is represented by rotations at the nodes; the flexion of an individual element is not considered. From the inertial viewpoint, the inclusion is treated as a set of lumped masses coinciding with the nodes. This rheological model is illustrated in Fig. 2.b.

### 2.3 *Intrinsic behaviour*

The magnitude of the tensile force in the q-th element is related to the elongation in eq. (1). This definition implies that the inclusion can carry tensile forces only (i.e. positive).

$$T^q = \max\left[J.\varepsilon^q\,;\,0\right] \tag{1}$$

The resultant force vector on an arbitrary node $q$ is the sum of the tensile force vectors $T_i^q$ and $T_i^{q+1}$ in elements $q$-1 and $q$. A gravitational forces $m^q g_i$ may also be considered, $m^q$ being the mass of node $q$. Consequently, the second Newton's law applied to node $q$ writes

$$\ddot{\mathbf{x}}_i^q = \left(T_i^{q-1} + T_i^q\right)/m^q + g_i \tag{2}$$

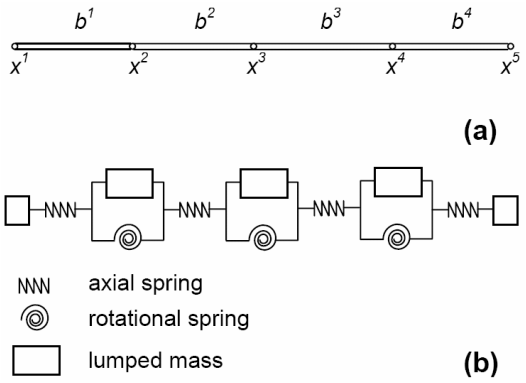


Figure 2. Discretization of an inclusion and associated inertial model.

### 2.4 *Mechanical coupling*

The constitutive behaviour of grain-inclusion contacts is defined by normal and tangential stiffnesses $k_n$ and $k_s$ and the friction angle $\delta$. Thus, contact forces can be computed from the relative displacements at contacts.

The DSEM is coupled with the DEM code by considering the grain-inclusion contact forces $f_i^k$ as external loads on the inclusion. Thus, if $n$ contacts exist on elements $q$-1 and $q$, eq. (2) becomes

$$\ddot{\mathbf{x}}_i^q = \left(T_i^{q-1} + T_i^q\right)/m^q + g_i + \sum_{k=1,\ldots,n} \xi^k f_i^k \tag{3}$$

were $\xi^k$ varies lineary between 1 and 0 when the position of contact point $k$ moves from node $q$ to node $q$+1.

For each contact, a forces $-f_i^k$ is introduced as an external load on the grain corresponding to contact $k$.

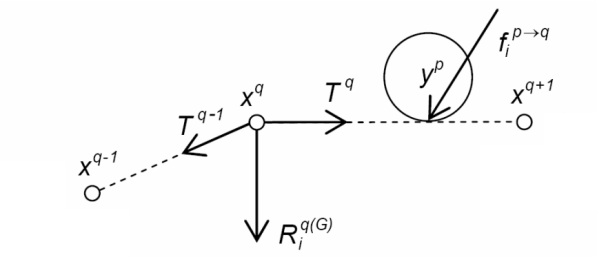


Figure 3. Different types of loads participating to the resultant force on a general node.

## 3 ANCHORAGE OF GEOSYNTHETICS : NUMERICAL VERSUS EXPERIMENTAL MODELLING

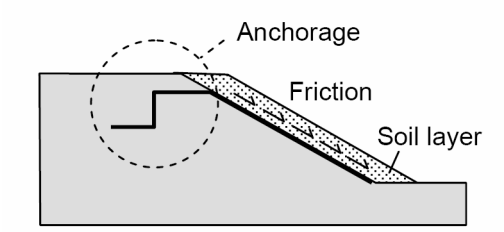


Figure 4. Anchorage of a geosynthetic lining system at the top of a slope.

### 3.1 *Anchorage of geosynthetics*

Geosynthetics are used as liner systems on slopes in a large number of geotechnical applications for reinforcement or watertightness purposes (canal banks, reservoirs, landfills, etc.). The stability of such systems depends on the efficiency of the anchorage at the top of the slope. That is why the geosynthetic sheets are often installed in trenches to ensure effective anchorage (see fig. 4). To design the system, it is necessary to estimate the tension that can be mobilised in the anchor (the anchoring capacity) as function of the geometry and the properties of the constituent materials. Due to complex features of failure, this estimation is still problematic.

A true scale pull-out apparatus (Fig. 5) has been developed at the CEMAGREF (research institute for agricultural and environmental engineering) in Bordeaux by Briançon (2000) to investigate the mechanical behaviour of anchorages. In this section, the results of predictive computations using the DEM-DSEM coupling are contrasted against a series of tests carried out at the CEMAGREF (the tests are reported in Chareyre et al. (2002)).

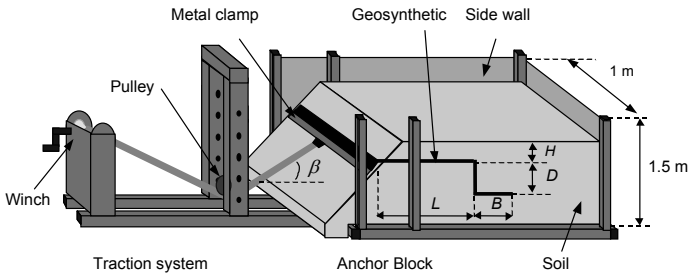


Figure 5. Pull-out apparatus of the CEMAGREF – Bordeaux.

### 3.2 *Modelling the actual behaviour of the materials at the macro-scale*

#### 3.2.1 *Soil : a macroscopic analogy*

The properties of the soils used in the pull-out tests (a sand and a silt) were measured in laboratory tests. The behavior of both soils was characterized considering a Mohr-Coulomb yield criterion, with cohesion $c$ and friction angle $\varphi$ (table 1).

Table 1. Properties of the soil used in the experiments.

| Parameter | Cohesion $c$ | Friction angle $\varphi$ | Density $\rho$ |
|---|---|---|---|
| | kPa | degree | kg.m$^{-3}$ |
| sand | 0 | 41 | $16.7\times10^3$ |
| sandy silt | 13 | 34 | $18.5\times10^3$ |

For the DEM modelling, it was decided to set the parameters of the contact laws so that the behaviour of the soils simulated is macroscopically equivalent to the behaviour of the soils used in the experiments. Clearly, there is no obvious method to do this at the present time. The method that was chosen is discussed in Chareyre (2001). It can be summarized as follows :

The particle size distribution (polydisperse) was fixed independently of the actual distribution. Biaxial compression tests were simulated to calibrate micro-macro relations in the particular case of the size distribution chosen. This calibration, together with dimensional analysis, enabled us to choose appropriate micro-parameters so that the biaxial tests simulated fit the behavior of the actual soil at the macro-scale (and at the macro-scale only). In figure 6, the results of biaxial simulations after the contact laws has been set are compared with the experimental failure criterion obtained for the sand.

Note that the soil was modelized with clusters (see Fig. 7) rather than single cylinders, to reach high values of internal friction angle. Each cluster was made of two discs with a slight difference in sizes (sizes ratio equal to 0.9). Clusters were generated in two different sizes, with a proportion of four small clusters for each large cluster (twice larger).

The cohesion in the DEM model was defined in terms of normal and tangential local cohesion, so that the tensile and shear strengths, $R_n$ and $R_s$, of a contact between two particles of diameters $d_i$ and $d_j$ is computed as

$$R_k = C_k.\min(d_i, d_j) \qquad k = n,s \tag{4}$$

Table 2. Parameters of the contact laws selected to simulate the behaviour of the actual soils at the macroscopic level (with $k_n$ and $k_s$ the normal and tangential stiffness, $\mu$ the angle of contact friction, $C_n$ and $C_s$ the normal and tangential local cohesion).

| Parameter | $k_n$ | $k_s$ | $\mu$ | $C_n$ | $C_s$ |
|---|---|---|---|---|---|
| | kPa | kPa | degree | kPa | kPa |
| sand | $5\times10^4$ | $2.5\times10^4$ | 38.7 | 0 | 0 |
| sandy silt | $1.5\times10^4$ | $0.75\times10^4$ | 32.6 | 192 | 96 |

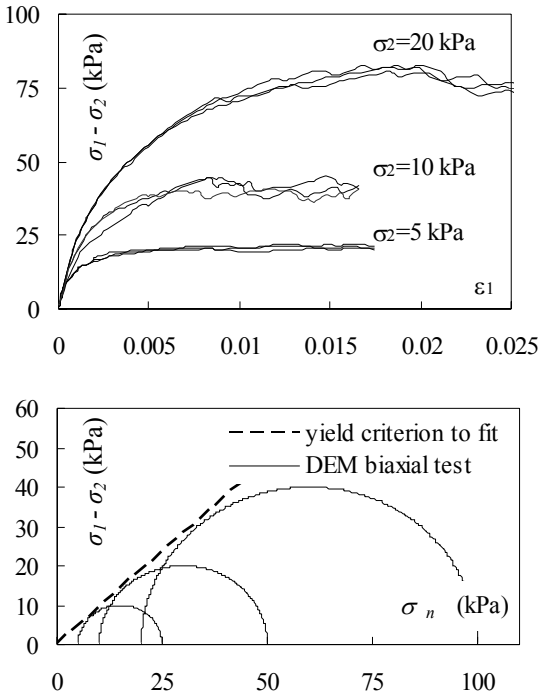


Figure 6. Stress-strain curves obtained after simulating biaxial compressions with the sand model (3 samples with 4000 clusters each) and comparison with experimental yield criterion.

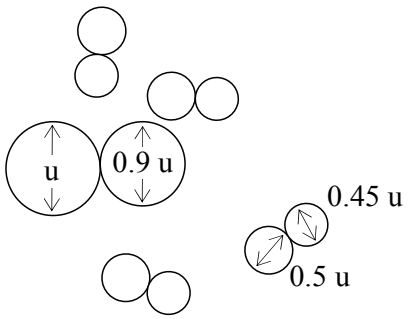


Figure 7. Clusters used to simulate the soil materials

#### 3.2.2 *Soil-inclusion interface*

The macroscopic friction ratio at the soil-inclusion interface was measured in shear tests. It was found equal to 34° (the value was the same for sand-inclusion or silt-inclusion interfaces).

In the DEM-DSEM coupling, the macroscopic interface friction simulated correspond to the local friction $\delta$, so that $\delta$ was defined directly from the results of the shear tests : 34°.

The stiffness of the soil-inclusion contacts was taken equal to the stiffness of the soil-soil contacts.

### 3.3 *Results*

One important result of the tests was that the failure mechanism was strongly influenced by the nature of the soil. A significant deformation was observed with the sand (Fig. 8) while far less deformation was observed in the silt (the failure being essentially due to slippage at the soil-inclusion interface in that case). Fig. 9 shows the geometry of the anchorage simulated, at initial state and after the pull-out simulation, with the parameters corresponding to the silt

(soil 1) and the sand (soil 2). The results are in good agreement with the experimental observations : little deformation of the silt, large deformation of the sand.

More important : the evolution of the tensile load $T$ during the pull-out process is correctly predicted by the simulations. Particularly, the maximum value of $T$, which defines the anchoring capacity, is predicted with a precision of 25%.

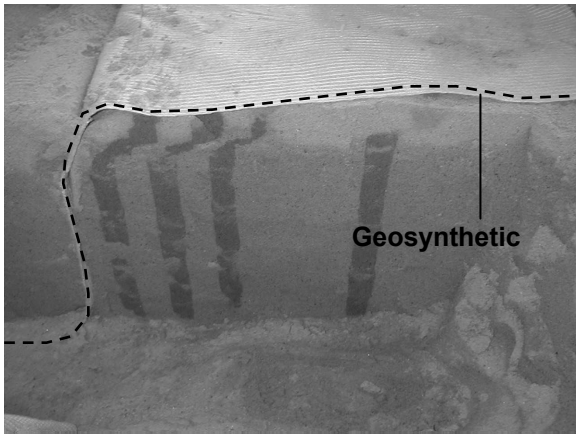


Figure 8. Deformation of the anchoring sand mass after the pull-out test evidenced by coloured sand columns (initially vertical).

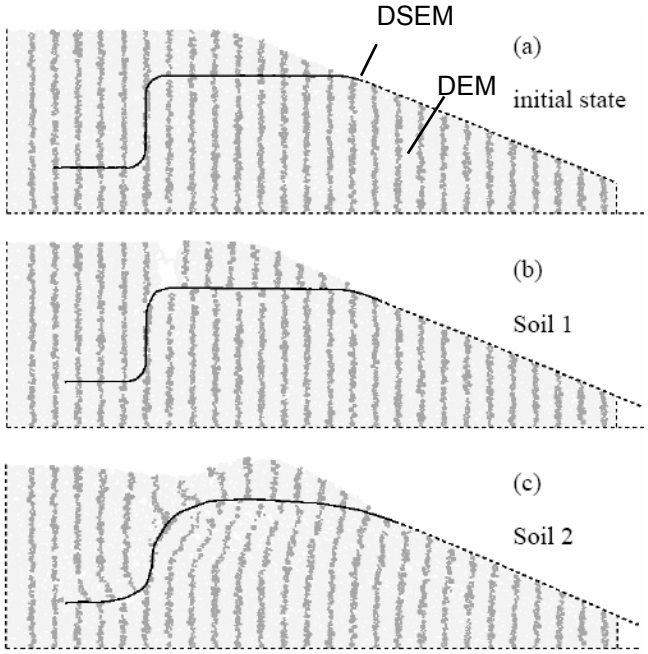


Figure 9. Initial state (a) and simulated evolution of L-shaped anchor with Soil 1 (b - silt) and Soil 2 (c - sand).

## 4 CONCLUSION

The DEM has been applied to investigate the behaviour of soil-geosynthetic structures at the macro-scale. The comparison with experimental data has shown that the proposed modelling can predict the behaviour of the system correctly.

This result suggests that the DEM can be applied in order to obtain some quantitative and predictive data concerning the behaviour of soil structures, even if the modelling implies an up-scaling of the particles' size.

It is believed that, compared to finite elements methods, the main advantage of the DEM is the robustness. The DEM can handle large deformations, localisation, loss/gain of contacts and multi-materials interfaces without major difficulty. Since all those features are present simultaneously in composite soil structures, the DEM could be particularly well suited in that case.

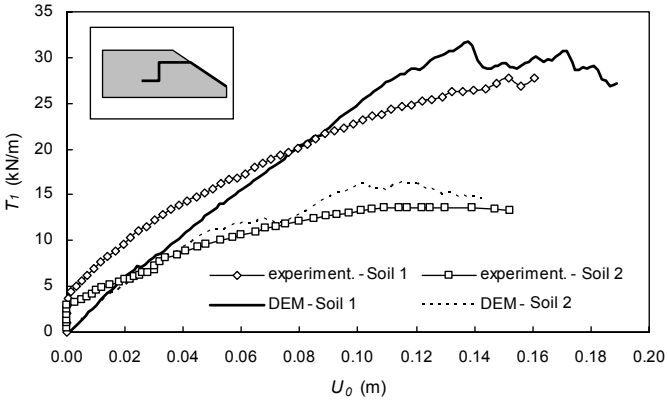


Figure 16. Comparison between the tests and the simulations for L-shaped anchor and both types of soil.

## REFERENCES


Briançon, L., Girard, H., Poulain, D., and Mazeau, N., 2000. "*Design of anchoring at the top of slopes for geomembrane lining systems"*. 2nd European geosynthetics conference, Bologna, Italy, 15-18 October 2000, 2: 645-650.

Chareyre, B., Briançon, L., and Villard, P., 2002. "Numerical versus experimental modelling of the anchorage capacity of geotextiles in trenches". *Geosynthetics International*, 9(2): 97-123.

Chareyre, B., and Villard, P., 2002. "*Discrete element modelling of curved geosynthetic anchorages with known macro-properties"*. Proc. of the First International PFC Symposium, Gelsenkirchen, Germany. 6/7 November 2002. Konietzky (ed): 197-203.

Chareyre, B., and Villard, P., 2005. "Dynamic Spar Elements and DEM in 2D for the modelling of soil-inclusion problems". *Journal of Engineering Mechanics - ASCE*. In press.

Cundall, P.A., Strack O.D.L. (1979). "A discrete numerical model for granular assemblies." *Geotechnique*, 29(1), 47-65.

Hart, R., Cundall, P.A., and Lemos, J. (1988). "Formulation of a three-dimensional distinct element model. II : Mechanical calculations for motion and interaction of a system composed of many polyhedral blocks." *Int. J. Rock Mech., Min. Sci. & Geomech. Abstr*., 25(3), 117-125.

Hentz, S., Daudeville, L., and Donze, F. (2003). "*Modeling of reinforced concrete structures subjected to impacts by the discrete element method.*" Proc., 16th Engineering Mechanics Conf. EM2003, ASCE, Seattle.

Mohammadi, S., Owen, D.R.J., and Peric, D. (1998). "A combined finite/discrete element algorithm for delamination analysis of composites." *Finite Elements in Analysis and Design*, 28(4), 321-336.

Villard, P., Kotake, N., and Otani, J., (2002). "*Modeling of reinforced soil in finite element analysis*." Keynote lecture, Proc., 7th International Conference on Geosynthetics, Gourc J.P. and Delmas P., eds., Nice, France, 39-95.